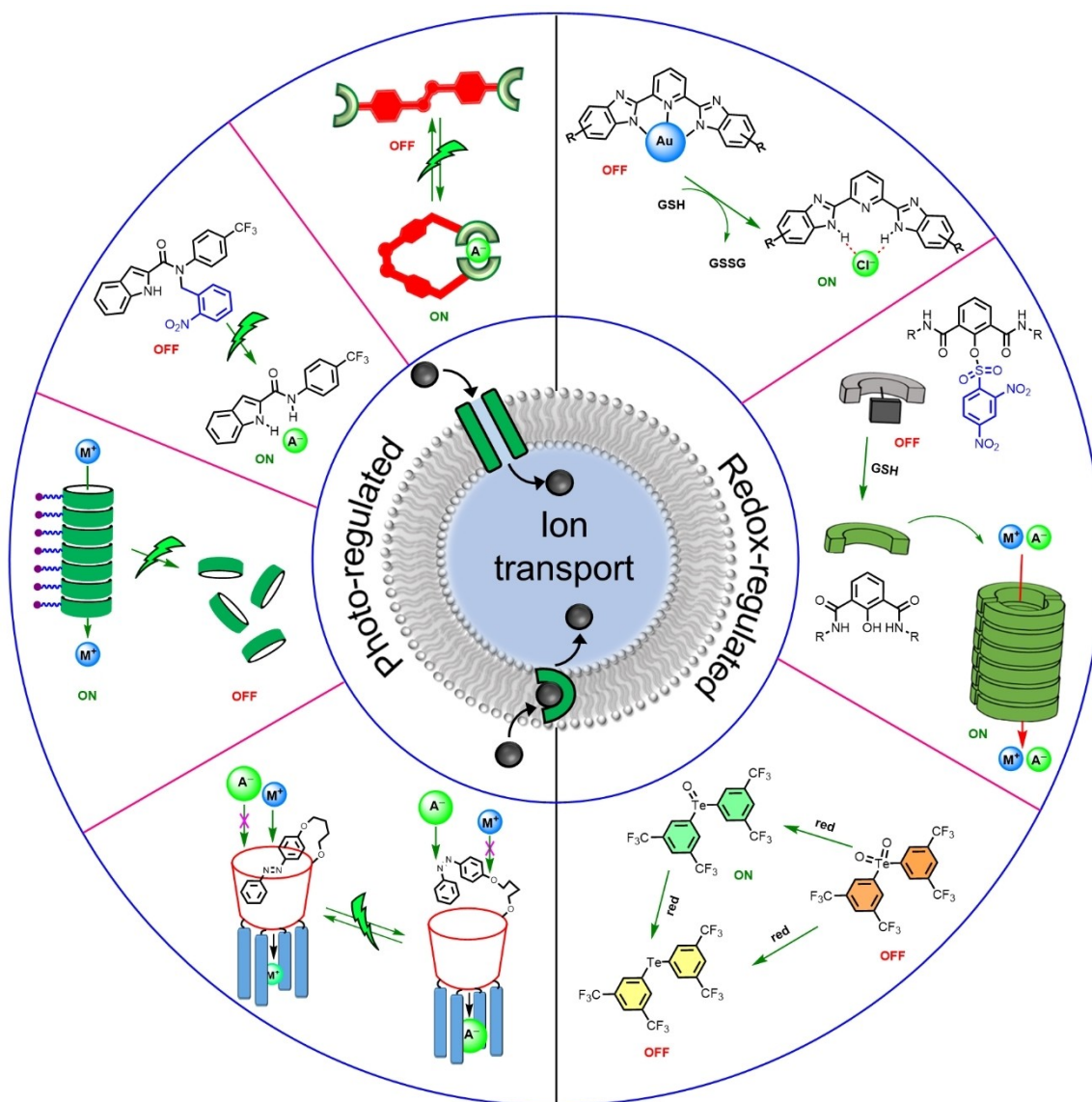


How to cite: *Angew. Chem. Int. Ed.* **2023**, 62, e202308842  
 doi.org/10.1002/anie.202308842

## Ion Channels

# Photo- and Redox-Regulated Transmembrane Ion Transporters

Manzoor Ahmad, Shaun A. Gartland, and Matthew J. Langton\*



**Abstract:** Synthetic supramolecular ion transporters find applications as potential therapeutics and as tools for engineering functional membranes. Stimuli-responsive systems enable external control over transport, which is necessary for targeted activation. The Minireview provides an overview of current approaches to developing stimuli-responsive ion transport systems, including channels and mobile carriers, that can be controlled using photo or redox inputs.

## 1. Introduction

The development of synthetic supramolecular ion transporters is an area of significant current interest, driven by potential applications in therapeutics for cancer and channelopathies (diseases arising from mis-regulated ion transport, such as cystic fibrosis), and to develop tools for chemical biology or for engineering functional membranes in artificial cells.<sup>[1]</sup> In nature, the transmembrane transport of ions is mediated by membrane protein channels and pumps.<sup>[2]</sup> A key feature is their ability to regulate transport in response to external stimuli, such as small molecule binding, membrane potential or light. Whilst the development of synthetic mobile ion carriers and channels is now well established, systems which can be regulated with external stimuli remain relatively rare, but have promise as spatiotemporally targeted probes and therapeutics. In recent years significant progress has been made in accessing both channel and carrier systems that can be controlled via external stimuli, including ligands,<sup>[3]</sup> pH,<sup>[4]</sup> voltage,<sup>[5]</sup> and enzymes<sup>[6]</sup> to switch on and off ion transport.<sup>[7]</sup> Amongst the range of external stimuli available, light and redox have attracted the most attention. Light is attractive due to the prospect of spatiotemporal activation using biocompatible wavelengths, and a wide range of switchable receptors for anions have been reported, some of which have been applied to regulating transport.<sup>[8]</sup> On the other hand, the development of redox responsive systems is motivated by targeting cellular redox environments such as reactive oxygen species and glutathione (both of which are increased during rapid proliferation of cancer cells, for example). In this mini review we highlight the various approaches through which photo- and redox-responsive behavior may be engineered into ion transport systems

## 2. Photo-Responsive Ion-Transport Systems

In the context of developing targeted ion transporters as therapeutics for channelopathies or to combat cancer by inducing chloride mediated apoptosis,<sup>[9]</sup> photo-responsive ion transport systems are of particular interest due to the

possibility of high spatio-temporal control, fast response time and low toxicity of the stimulus.<sup>[10]</sup> In the following section we will outline the various approaches to integrating photo-responsive behavior into ion channels and carriers.

### 2.1. Ion Transporters with Irreversible Photo-controlled Activity

Molecular self-assembly of small monomer units within a lipid bilayer membrane is a common strategy to generate artificial ion channel structures, and photo-responsive components have been used to control this assembly and disassembly process. Talukdar and co-workers reported such an approach by developing irreversibly photo-gated ion channels utilizing a fumaramide self-assembling unit (Figure 1).<sup>[11]</sup> The fumaramide derivatives **1a–5a** efficiently self-assemble into barrel-rosette ion channels via multiple intermolecular hydrogen bonding interactions. In contrast, the corresponding maleimide-based systems **1b–5b** were found to be less active, which was suggested to be due to intramolecular-hydrogen bond structural locking leading to poor self-assembly. Photo-irradiation of the fumaramide channel with UV light greatly reduced the ion transport activity by triggering photoisomerization into the maleimide-based structure and disassembly of the channel.

The concept was further extended to generate cholic acid-based light-responsive barrel stave ion channels (Figure 2).<sup>[12]</sup> Cholic acid provides a hydrophobic backbone to enhance interactions with the lipid bilayer membrane and a hydrophilic domain necessary for the recognition of ions

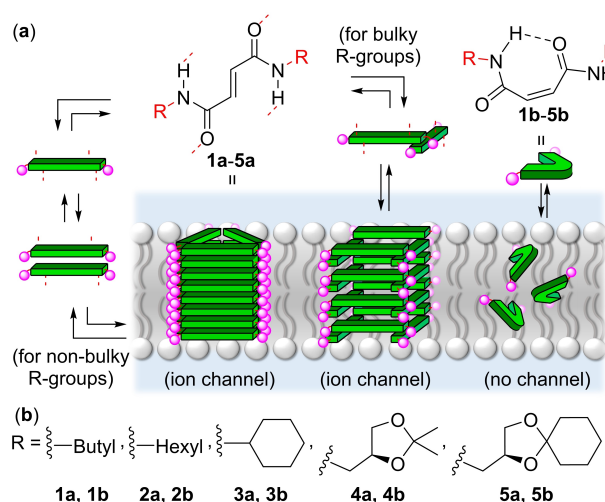


**Figure 1.** (a) Schematic representation of the self-assembly processes of fumaramides **1a–5a** and maleamides **1b–5b** in the lipid bilayer membrane and (b) structure of the hydrophobic tails.

[\*] Dr. M. Ahmad, S. A. Gartland, Prof. M. J. Langton  
Department of Chemistry, University of Oxford, Chemistry Research  
Laboratory  
Mansfield Road, Oxford OX1 3TA (UK)  
E-mail: matthew.langton@chem.ox.ac.uk

© 2023 The Authors. Angewandte Chemie International Edition published by Wiley-VCH GmbH. This is an open access article under the terms of the Creative Commons Attribution License, which permits use, distribution and reproduction in any medium, provided the original work is properly cited.

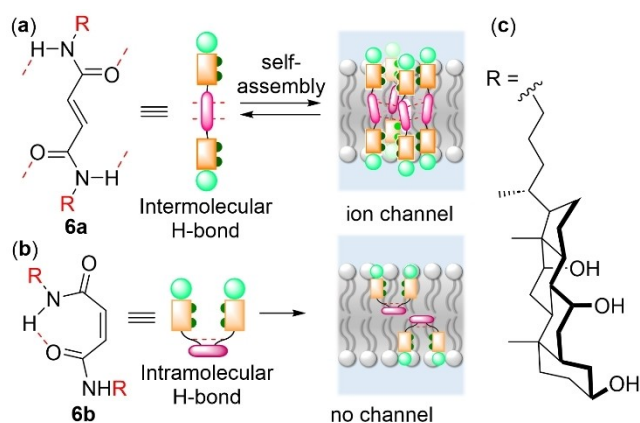


**Figure 2.** (a) Schematic representation of the self-assembly processes of fumaramide **6a** and, (b) maleimide **6b**, in a membrane phase. (c) Cholic acid derived substituent.

within the channel. The fumaramide-based ion channels **6a** were found to be more active compared to the corresponding maleimide-based ion channels **6b**, whilst photo-irradiation with UV light of the former significantly diminished the ion transport activity of these channels, likely due to the formation of the inactive maleimide. However, in this system isomerization back to the active furamide state could not be achieved due to the formation of stable intramolecular hydrogen bonding.

The concept of irreversible activation has also been applied to mobile ion carriers. Photocages are versatile motifs that offer a method to generate an in-active substrate that can be activated with light. *Ortho*-nitrobenzyl (ONB) derivatives in particular have been extensively explored for

applications including the activation of anticancer drugs,<sup>[13]</sup> and recently have been used to photocage protein ion channels. For example, Koçer et al. incorporated an ONB-based photocage into an MSC1 protein channel to photo-modulate ion channel activity.<sup>[14]</sup> Photocaged artificial carriers and channels offer a complementary, synthetically versatile approach compared to the complexities of derivatizing naturally occurring channels. In this regard, Zhu and co-workers developed ONB-caged benzo crown ether ion channel monomers **7a** and **7b** (Figure 3).<sup>[15]</sup> Monomer **7b** was found to be more active compared to **7a** ( $EC_{50}$  of 3.4 mol % and 10.3 mol % with respect to lipid, respectively). Channel formation was confirmed via patch-clamp experiments in which well-defined channel opening and closing behavior was observed with the conductance values of 0.25 and 0.40 nS for **7a** and **7b**. Photo-irradiation at 365 nm significantly decreased the ion transport activity due to cleavage of the ONB cage and the disruption of ion channel structure within the membrane.

Exploiting a mobile carrier approach, Talukdar and co-workers developed an ONB-linked indole-2-carboxamide-based anionophore that could be photoactivated inside both artificial liposomes and cancer cells to induce chloride-mediated apoptosis (Figure 4).<sup>[16]</sup> Incorporation of an ONB-photocage to the amide binding site of the indole-2-carboxamide receptor **9** drastically reduces the ion transport activity by blocking one of the two H-bond donors and inhibiting anion binding. Photoirradiation at 365 nm to cleave the ONB-cage, re-generates the active transporter. Such photoactivation also induced chloride-mediated apoptosis inside the MCF-7 cancer cells, pointing to future applications within photo-targeted cancer therapies.



Manzoor completed his B. Sc. (2011) and M. Sc. (2014, Organic Chemistry) from the University of Kashmir. He completed his DPhil (2022) with Prof. Pinaki Talukdar at IISER Pune on the topic: "Development of Biomimetic Photo-Responsive Artificial Carriers for the Transmembrane Chloride Transport". He is currently a PDRA in the Langton group working on stimuli-responsive ion transporters.



Shaun Gartland received his MChem degree from the University of York in 2020, where he carried out a research placement at the Lubrizol Corporation. He is currently a DPhil student at the University of Oxford, researching photocaged cationophores for transmembrane cation transport.



Matthew Langton obtained his MChem at the University of Oxford, where he remained in Oxford for a DPhil (PhD) under the supervision of Prof. Paul Beer, before moving to the University of Cambridge to take up an Oppenheimer Early Career Fellowship in the group of Prof Chris Hunter FRS. He started his independent career in Oxford in 2018 as a Royal Society University Research Fellow, where he is now Associate Professor and Fellow of Balliol College. His research interests are in supramolecular chemistry and coordination chemistry.



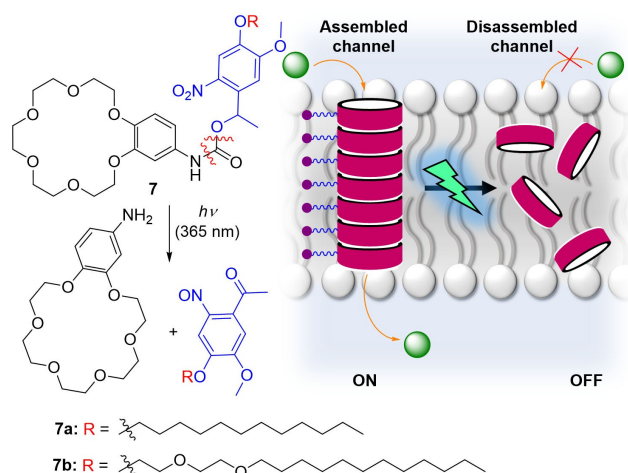


**Figure 3.** Chemical structure, schematic representation of channel-like self-assembly of ONB-caged compound **7** for cation transport, and its proposed photo-deactivation mechanism.

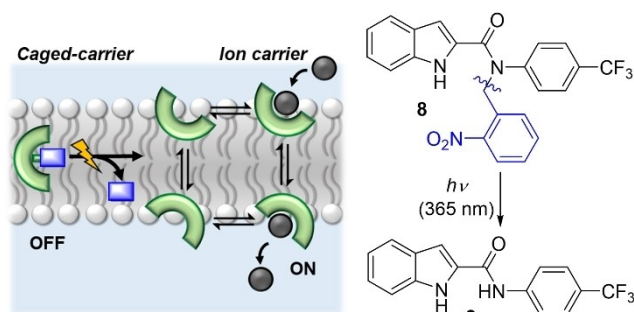


**Figure 4.** Photo-triggered release of an anion carrier **9** from the corresponding ONB-caged pro-carrier **8**.

Langton and co-workers recently demonstrated an alternative approach to controlling the activity of an ion carrier by modulating its mobility across the lipid bilayer membrane (Figure 5).<sup>[17]</sup> Squaramide and triazole derived ion carriers were appended to a dodecyl-based membrane-targeting anchor through an ONB-based photo-cleavable linker. The activities of the free carriers **10** and **11** were inhibited upon attachment to the anchor due to diminished mobility within the membrane, while in situ photoirradiation of the anchored carriers within the membrane to remove the anchor led to activation of transport. Differing from blocking the binding site to inhibit transport, this approach involves remote functionalization of a transporter without de-novo binding site design, so has potential to be applicable to photo-caging a wide range of existing ion carrier designs.

In a different approach, Khairutdinov and Hurst developed a crown ether tethered spiropyran-based  $K^+$  transporter **12** (Figure 6) in which the polarity, and hence ability to access the membrane interface, could be modulated.<sup>[18]</sup> Spiropyran may be switched between the ring-closed neutral (spiro) form, and ring-open charged (merocyanin form) using UV and visible light. In this case, the ring-open, more polar merocyanin form was found to be more active than

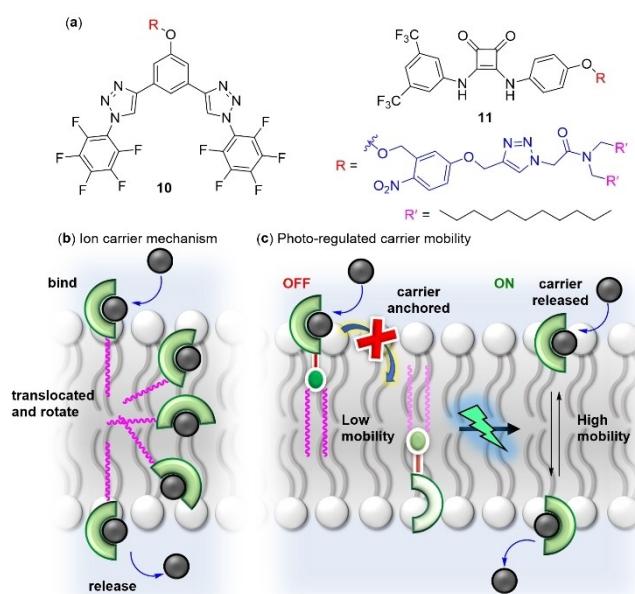


**Figure 5.** (a) Membrane-anchored pro-carriers **10** and **11**. (b) Mechanism of ion transport by a carrier mechanism, and (c) mechanism of photo-regulated ion transport by controlling carrier mobility.

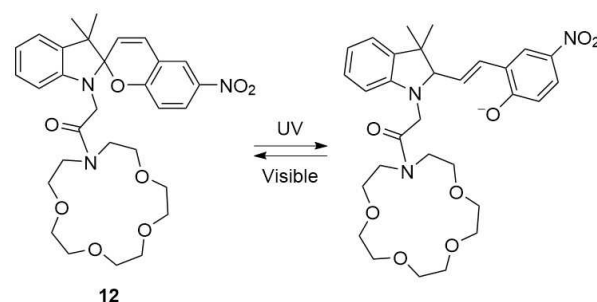


**Figure 6.** Photo-regulated cation transport by a crown ether tethered spiropyran photoswitch **12**.

the spiro form, which was hypothesized to be due to the latter being confined within the hydrophobic lipid interior, and less able to access the polar interface region.

## 2.2. Reversibly Controlled Transporters with Differential Ion Affinity

Ion binding at the membrane-aqueous interface is requisite to facilitate transport by a mobile carrier. Accordingly, one approach to develop photo-responsive transporters is to modulate ion binding affinity between two photo-isomeric forms of a switchable carrier, by exploiting changes in molecular geometry, binding site accessibility and cooperativity. Azobenzene is a commonly used photoswitch which exhibits a significant change in geometry and dipole moment upon *E-Z* photoisomerization, and has found wide-ranging applications, including in molecular electronics, data storage and photo-reversible ion sensing.<sup>[19]</sup> Such applications sug-

gest their potential efficacy in photo-responsive ion transport systems. In this regard, Jeong and co-workers in 2014 reported an azobenzene-based photoresponsive chloride anion transport system containing two urea or thiourea anion binding motifs, connected through an azobenzene subunit (Figure 7, compound **13**, R=H, X=O or S).<sup>[20]</sup> The thermodynamically stable *E* isomer was found to be less active compared to the *Z* isomer. This enhanced ion transport activity was attributed to the efficient anion binding in the *Z* form in which both hydrogen bond donor sites can cooperatively bind the anion. However, no reversible in situ switching of anion transport activity was achieved with this system.

In a related approach, Talukdar and co-workers reported a sandwich-shaped azobenzene-based diamide dimer **15** as a

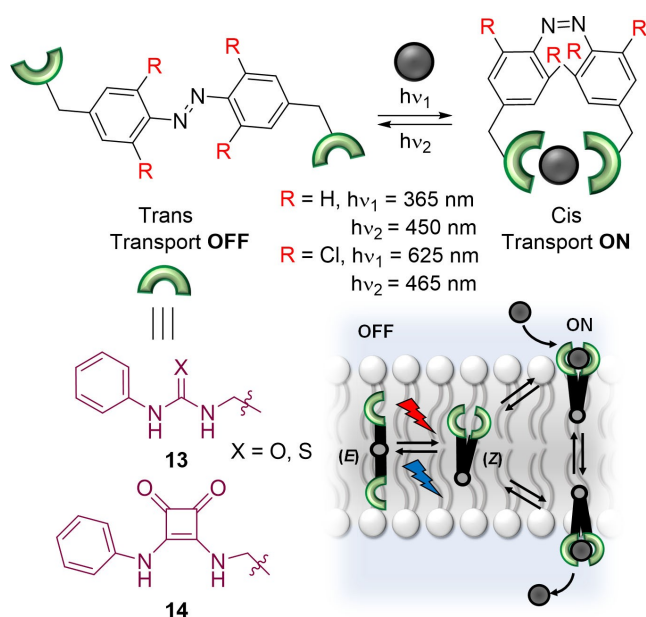


**Figure 7.** Photo-regulated anion transport by azobenzene-based mobile carriers containing urea, thiourea, and squaramide anion binding motifs.

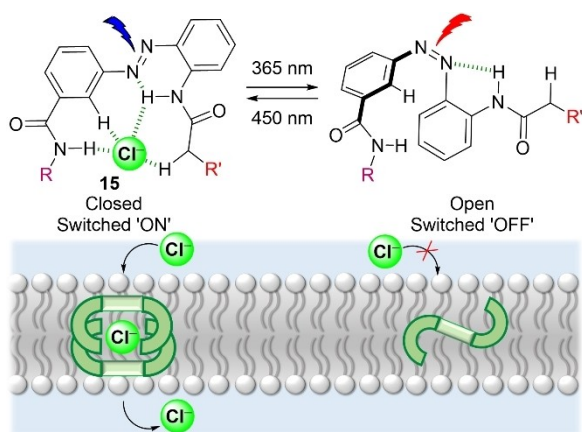


**Figure 8.** Design and working principle of azobenzene-based photo-regulated ion transporter **15**.

photoresponsive ion carrier (Figure 8).<sup>[21]</sup> Here the *E* isomer exhibited efficient ion binding and transport activities due to the closed structure and proximity of anion-binding amide moieties. The photo-isomerized *Z* state, on the other hand, was observed to be less active because of its open structure that led to weak anion binding and hence poor transport activities. The enhanced activity in the *E* isomer was further attributed to the formation of a sandwich-shaped chloride-bound active ion transport complex that completely encapsulates the chloride anion, which is necessary for improved membrane permeation. Photo-reversible ion transport activities were achieved over many cycles upon alternative photo-irradiation using 365 nm and 450 nm of light respectively.

The systems discussed above are triggered using UV light. However, for biological applications visible or near-IR activation is preferable due to enhanced tissue penetration and minimized phototoxicity.<sup>[22]</sup> In this regard, Langton and co-workers developed an azobenzene-based photo-responsive ion transport system that is reversibly isomerized using visible light (Figure 7, compound **14**, R=Cl).<sup>[23]</sup> The system contained two squaramide anion receptors interconnected through a tetra-chloro *ortho*-substituted azobenzene with red-shifted  $n-\pi^*$  absorption bands. *E* to *Z* photo-isomerization with red light enhanced anion binding and transport (by a factor of 8 with respect to the *E* isomer), due to cooperative binding of chloride by the two squaramide H-bond donors, whilst the reverse process could be achieved using blue light. The extended conformation of the *E* was postulated to lead to poor membrane mobility, whilst molecular dynamics simulations suggested that dimerization within the membrane may also contribute to the low activity of the *E* isomer.<sup>[24]</sup> Subsequent work demonstrated that subtle changes in structure of the transporters could be used to enhance the overall activity, or modulate the switching wavelengths by modifying the azo core.<sup>[24]</sup>

Stiff-stilbenes are molecular photoswitches that can be reversibly interconverted between the *E* and *Z* isomers using UV/Visible light.<sup>[25]</sup> The *E* isomer is a more elongated open structure while the *Z* isomer exists as a closed conformation. Such structural differences have been exploited to generate photo-reversible anion receptors.<sup>[25]</sup> Wezenberg, Gale and co-workers utilized this concept to develop photo-responsive anion transporter **16** in which two anion binding thiourea moieties were connected to the two ends of a stiff-stilbene photo-switch (Figure 9).<sup>[26]</sup> In the *E* form, weak anion binding and poor ion transport were observed compared to the *Z* isomer. As with previous azobenzene systems, this was rationalized to be due to a combination of cooperative binding of the two thiourea moieties in the *Z* isomer, and poor activity of the *E* isomer due to the elongated and open structure. Reversible OFF-ON ion transport and, for the first time, photo-controlled membrane depolarization was achieved by alternating UV and visible light irradiation.

Acyhydrazones are another class of photo-switch based around the *E-Z* isomerization of C=N double bonds. The *Z* isomer of the pyridine derivatives in particular exhibit excellent thermal stability due to six-membered intramolec-

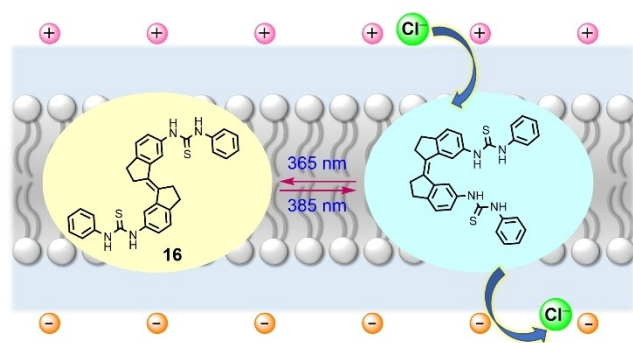


**Figure 9.** Design and working principle of stiff stilbene-based synthetic ion transporter **16** capable of chloride transport and membrane depolarisation.

ular hydrogen bonding. For this reason, they have found applications as photo-regulated molecular shuttles, in supramolecular self-assembly, and for photo-responsive ion sensing.<sup>[27]</sup> In 2022, Talukdar and co-workers reported an acyl hydrazone-based stimuli-responsive ion transport system **17** containing 5-(pentyloxy) isophthalic bis-carboxamide as an anion binding motif and 2-pyridyl acylhydrazone as a photoswitch (Figure 10).<sup>[28]</sup> The ion carriers showed efficient ion binding and transport activities as the *E* isomer, whilst anion binding and transport activities were attenuated by around 80 % upon photo-isomerization using 312 nm light. The active *E* isomer could be regenerated using

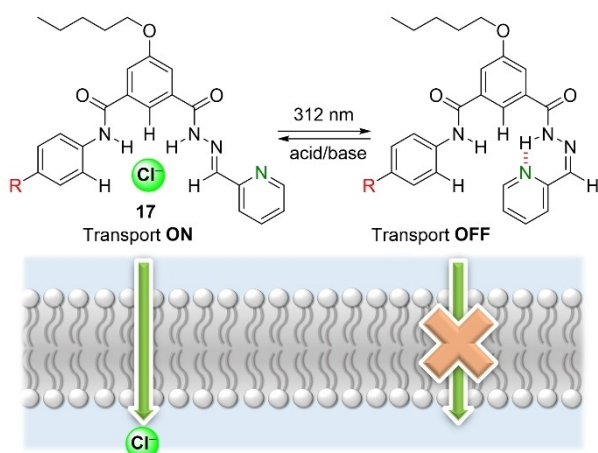


**Figure 10.** Acylhydrazone-based photo-regulated transporter **17**.

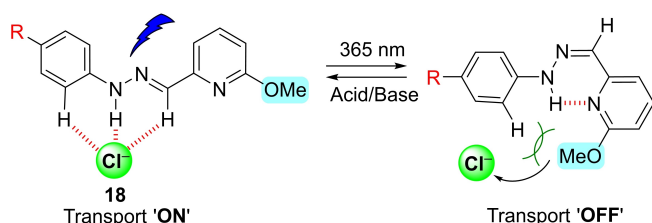


**Figure 11.** Phenylhydrazone-based photo-responsive ionophore **18**.

trifluoroacetic acid as a stimulus. The decrease in the activity in the *Z*-state was attributed to the blockage of the anion-binding site due to the formation of six-membered intramolecular hydrogen bonding. Such reversibly gated ion transport activity triggered by both light and acid/base stimuli could be repeated over numerous cycles.

Recently, the same group developed phenylhydrazone-based photoresponsive ion carrier **18** (Figure 11).<sup>[29]</sup> Phenylhydrazones also possess thermally stable *Z* isomers due to intramolecular hydrogen bond stabilization, however, unlike acylhydrazones ( $\lambda_{\text{max}} \approx 312$  nm), they absorb at comparatively higher wavelengths ( $\lambda_{\text{max}} \approx 365$  nm). Similarly, the *E* isomer could transport anions with low micromolar activity, which was inhibited in the *Z* isomer. This deactivation was rationalized as due to blocking of the anion binding site due to the formation of six-membered intramolecular hydrogen bonding, similar to that observed in acylhydrazone systems. Reversible deactivation and activation of ion transport activity was achieved by the application of light (365 nm, for *E* to *Z* isomerization) and acid stimulus (for *Z* to *E*), respectively.

### 2.3. Reversibly Controlled Transporters Exploiting Molecular Self-Assembly

Molecular photoswitches have also been used to control the self-assembly and disassembly of ion channels in a reversible fashion using two different wavelengths of light. Zhu and co-workers have developed one such example, consisting of an azobenzene-based photo-reversible ion channel with three crown ether macrocycle hydrophiles at alternate positions to the two azobenzene subunits **19** (Figure 12).<sup>[30]</sup> The ion channel structure furnished excellent cation transport in the *E-E* form, which was greatly diminished upon photoisomerization to the *Z-Z* state using 365 nm light, and reversed to regenerate the active *E-E* state using 450 nm light.

Zhu and co-workers in 2013 reported a similar type of azobenzene-based self-assembled photoresponsive cation channel (Figure 13).<sup>[31]</sup> A benzo-18-crown-6 derivative **20** was attached to a long amphiphilic alkyl chain through an azobenzene photo-switch to generate self-assembled supramolecular ion channel structures. The *trans* channels

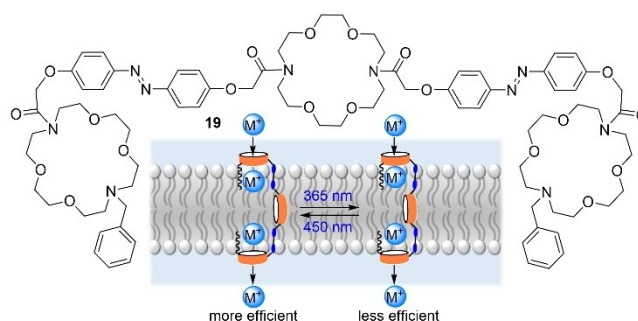


**Figure 12.** Design and working principle of azobenzene containing crown ether based cation channel **19**.



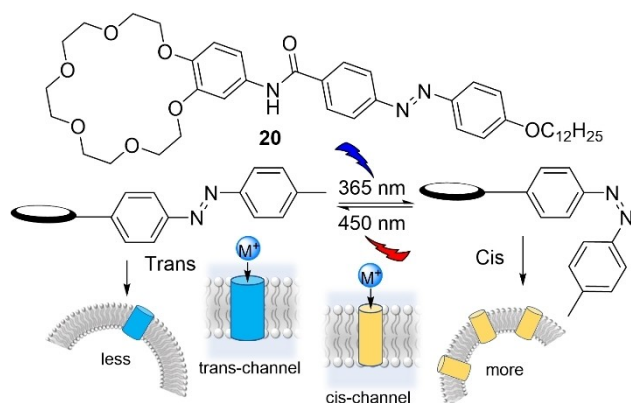


**Figure 13.** Molecular structure of channel-forming monomer **20** and schematic representation of the light-regulated ion channel transport.

yielded a conductance of 40 pA with a pore size of 5.8 Å, while the *cis* channels yielded a reduced ion current of 19 pA with a pore size of 2.8 Å. Photo-irradiation at 365 nm and 450 nm led to significant changes in the single channel ionic conductance due to the transformation of *trans* channels into the *cis* channels and vice-versa. In contrast, the *cis* channel was found to be over one order of magnitude more active compared to the *trans* form in bulk ion transport assays in vesicles. This was suggested to be due to the strong self-assembly behavior of the *trans* form in the aqueous phase leading to aggregation and hence a decrease in ion transport activity compared to the comparatively less aggregating *cis* form.

G-quadruplex, a secondary structure that exists in guanosine-rich nucleic acids, has been utilized to develop artificial ion channels which assemble in the presence of cations.<sup>[32]</sup> The formation of a G-quadruplex structure can also be controlled by triggering reversible conformational changes using external stimuli, including temperature, pH, light and molecular recognition.<sup>[33]</sup> Photoswitches such as azobenzene have been widely used to develop G-quadruplex-based bioinspired photo-responsive nano channels.<sup>[34]</sup> For example, Liu and co-workers developed an azobenzene-connected G-quadruplex photo-responsive ion channel **21**,<sup>[35]</sup> exhibiting efficient ion transport activities in the *E* isomer in which the G-quadruplex structure is stable (Figure 14). Photo-irradiation at 365 nm to generate the non-planar *Z* isomer disrupts the G-quadruplex and suppresses ion transport. The active *E* state could be regenerated using visible light irradiation at 450 nm, and repeated over many cycles.

Acylhydrazone photoswitches, in addition to their role in mobile carriers discussed previously, have also been utilized to control the self-assembly behavior of ion channels. For example, Liu and co-workers developed acylhydrazone-based self-assembled ion channels based on arylhydrazone crown ether triad structure **22** (Figure 15).<sup>[36]</sup> Three crown ether-appended hydrazine moieties were coupled to cyclohexane tricarboxylic acid to generate channels as the *E* isomer, assisted via multiple intermolecular hydrogen bonding interactions. Photo-irradiation at 312 nm to trigger *E-Z*

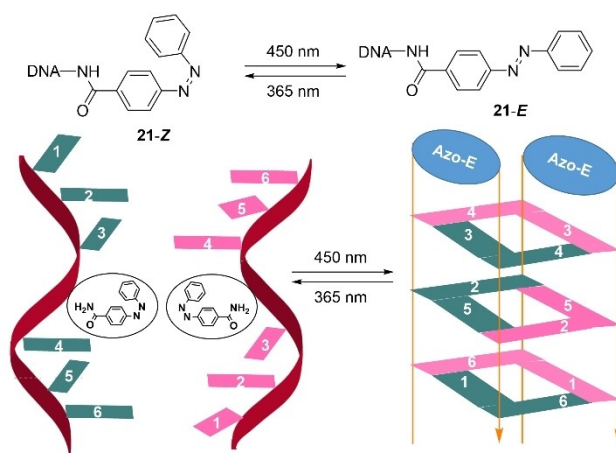


**Figure 14.** Photo-responsive G-quadruplex transmembrane channel **21**.

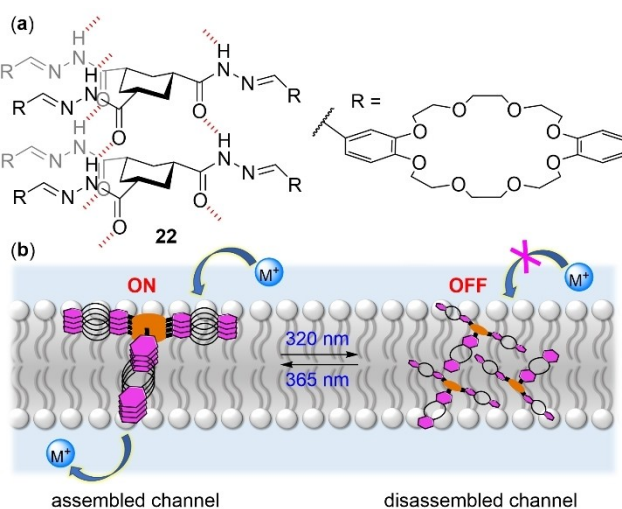


**Figure 15.** (a) Schematic representation of the assembly of **22-E** induced by the intermolecular hydrogen bonding. (b) Mechanism of photo-regulated transmembrane transport by acylhydrazone photo-switching.

isomerization disassembled the ion channel structure, while the initial self-assembled form could be subsequently regenerated by irradiation at 365 nm.

#### 2.4. Reversibly Controlled Transporters Exploiting Channel Blocking or Molecular Motion

In gated protein ion channels, an external stimulus leads to global conformational changes and the opening and closing of the channel.<sup>[37]</sup> The first attempt to make synthetic analogues of such systems was reported by Salzer and co-workers, who prepared a tetrakis(*p*-phenylazophenylaminomethyl)-cavitand with four axial azobenzene molecular photoswitches.<sup>[38]</sup> The group subsequently developed a related system with two axial azobenzene subunits (**23**), with the aim of accessing a photoresponsive ion channel structure (Figure 16).<sup>[39]</sup> Single

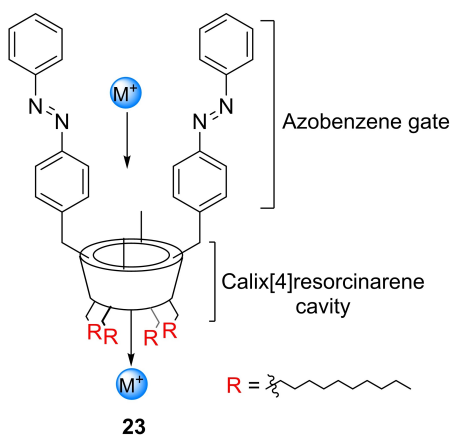


**Figure 16.** Azobenzene-containing calix[4]resorcinarene **23** as a photo-responsive ion channel.

channel conductance behaviour characteristic of an ion channel was observed for the *trans* form of the channels, but whilst photo-isomerisation in solution was possible, no switching of ion transport with light was achieved in this work. In a similar concept, Woolley and co-workers in 1996 developed azobenzene-based gramicidin peptide ion channels whereby light modulates the opening and closing of gramicidin pore (Figure 17).<sup>[40]</sup> Two molecules, 4,4'-bis(aminomethyl)azobenzene **24** and 3,3'-bis(aminometh-

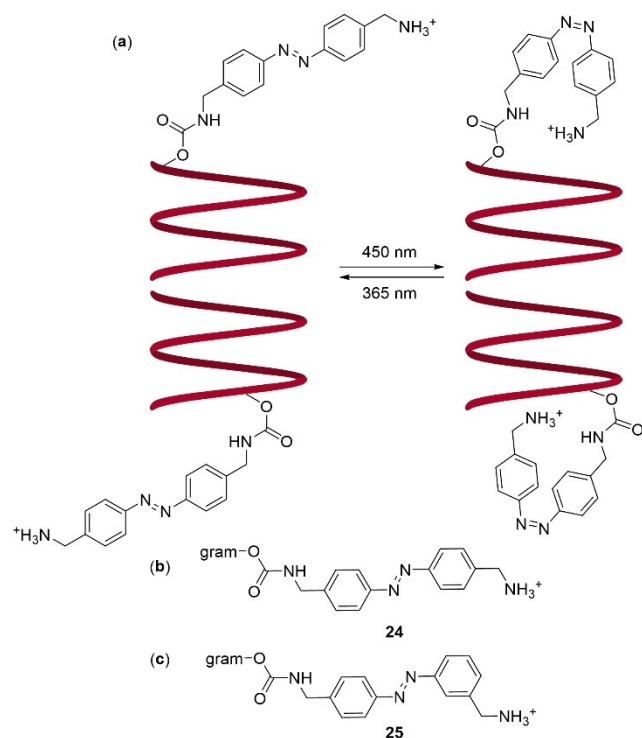


**Figure 17.** (a) Structure of azobenzene-modified gramicidin channels, shown in the *trans/trans* and *cis/cis* states. The gates are flexible and only one of several possible conformations is shown. (b) Covalent structure of the *para*-azobenzene “gate” and (c) the *meta*-azobenzene “gate”.

yl)azobenzene **25** were synthesized to form *trans-meta*-azobenzene-modified gramicidin and *trans-para*-azobenzene-modified gramicidin, respectively. Significant differences in the ion currents were observed upon the application of light only for *trans-meta*-azobenzene-modified gramicidin channels having *cis* carbamate linkage, with single channel conductance values of 14.9 and 12.8 pA for the *trans-trans* and *cis-cis* forms, respectively.

Later, Gin and co-workers developed an azobenzene-based ion channel working on a similar channel blocking principle (Figure 18).<sup>[41]</sup> The system contained an azobenzene photo-switch appended within a macrocycle (**26**) such that *E* isomer binds within the macrocycle and inhibits ion transport. Photo-isomerization to the *Z* isomer which is unable to bind with the macrocycle led to an increase in the anion transport and a decrease in the cation transport, respectively. This gating behavior was achieved reversibly over many cycles using 365 nm and 450 nm light, respectively.

Molecular machines in biological systems are structures that convert optical, chemical, or electrical energy into the mechanical work.<sup>[42]</sup> Developing artificial analogues is a thriving area of current research,<sup>[43]</sup> and in particular rotaxanes and catenanes have emerged as a powerful scaffold for controlling molecular motion in a stimuli-responsive manner.<sup>[44]</sup> Qu and co-workers have utilized the molecular motion of a macrocycle along a rotaxane's axle to transport  $K^+$  across lipid bilayer membranes.<sup>[45]</sup> They subsequently incorporated an azobenzene unit into the axle **27** to photo-modulate its shuttling behavior, and hence cation transport capability (Figure 19).<sup>[46]</sup> The *E* isomer was found to be around 5 times more active compared to the *Z* isomer, which was rationalized by the faster shuttling of the crown ether macrocycle along the axle, which is inhibited in the non-planar *Z* state.

Langton and co-workers recently developed a photo-responsive ion transport system based on a relay mechanism, in which transmembrane anion transport occurs by the transfer of anions between transporters present in the

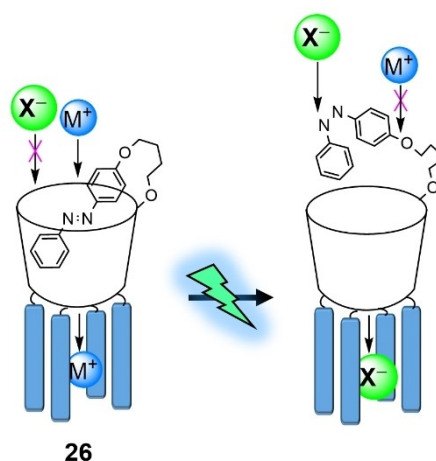


**Figure 18.** Schematic representation of anion and cation transport through an azobenzene-based photo-gated synthetic ion channel.



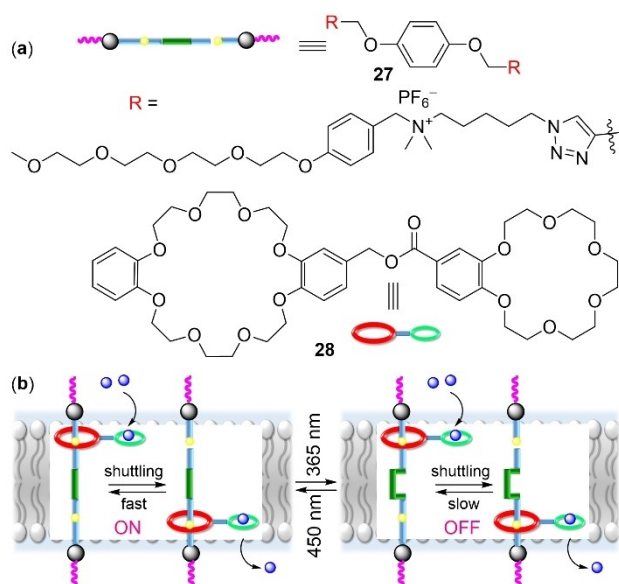


**Figure 19.** (a) Rotaxane-based molecular shuttle and (b) proposed mechanism for light-gated ion transport.

opposite leaflets of the bilayer (Figure 20).<sup>[47]</sup> The anion transport could be photo-reversibly controlled by incorporating a red-shifted azobenzene-based “telescopic” arm, reminiscent of a machine-like relay system. Efficient transport occurs only in the *E* isomer of **29** because the extended conformation is sufficiently long to facilitate transfer of the ion to a transporter located in the opposite leaflet. In contrast, in the *Z* isomer, the arm is too contracted reach into the center of the membrane and hence a significant reduction in anion transport activity was observed. The reversibly gated anion transport process could be reversibly controlled using green and blue light.

Molecular rotary motors are a class of molecular machines that undergo unidirectional motion under photo-irradiation, and which have found numerous applications in self-assembled and nanostructured materials, catalysis, and molecular electronics.<sup>[48]</sup> Tour and co-workers have utilized

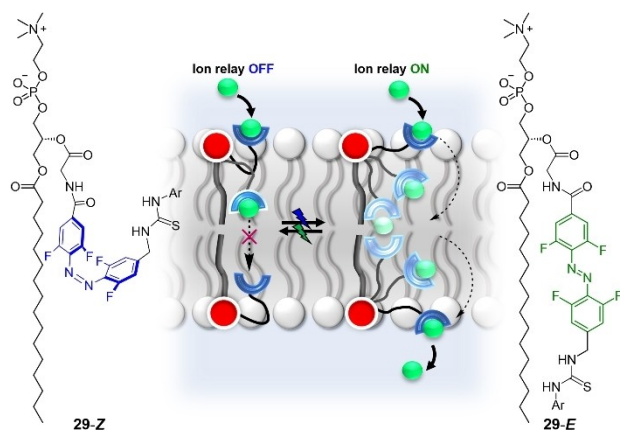


**Figure 20.** Photo-responsive transmembrane relay ion transporter **29**.

such systems to generate “molecular drills” which can be incorporated into the cell membrane and trigger cell death by permeabilizing the bilayer.<sup>[49]</sup> This type of rotary molecular motion has also been exploited to develop ion-selective channel structures. Barboiu, Giuseppone and co-workers utilized a light-driven rotary motor **30** to develop a photo-responsive cation channel in which two 18-crown-6 macrocycles were appended to a molecular rotor to generate an alkali metal cation selective channel structure within a lipid membrane (Figure 21).<sup>[50]</sup> Remarkably, ion transport was significantly enhanced upon continuous UV irradiation which was suggested to arise from the enhanced translocation of ions between the macrocycle units upon rotation of the rotor.

Bao and co-workers recently demonstrated a similar concept in which two benzo 18-crown-6 moieties were connected to the two extreme ends of the central rotary motor resulting in the formation of a  $K^+$  selective ion channel (Figure 22).<sup>[51]</sup> Photo-irradiation with UV light to trigger rotation of the motor significantly enhanced  $K^+$  ion transport activity, which was shown to induced caspase-dependent apoptosis of cancer cells.

### 3. Redox-Regulated Ion Transport

While photo-responsive transporters are to date arguably further developed, significant recent research effort has been dedicated to the study of redox-regulated transmembrane ion transport. This is motivated by the desire to activate ionophores and generate potential therapeutic transport systems that are activated in response to the cellular redox environment. In particular, a number of systems have now been developed that are activated by the reducing agent glutathione (GSH), which is present in elevated concentrations in cancer cells. One longer term aim here is to target activation to the specific redox window of a cancerous tumor, such that transmembrane ion transport disrupts ion homeostasis, and induces apoptosis, only in the tumor environment.

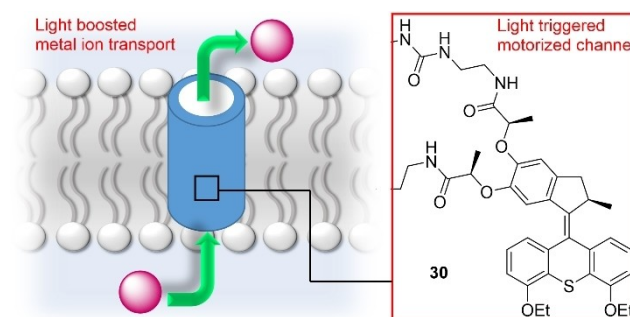


**Figure 21.** Schematic representation of cation transport mediated by photo-driven molecular motor-based ion channels.

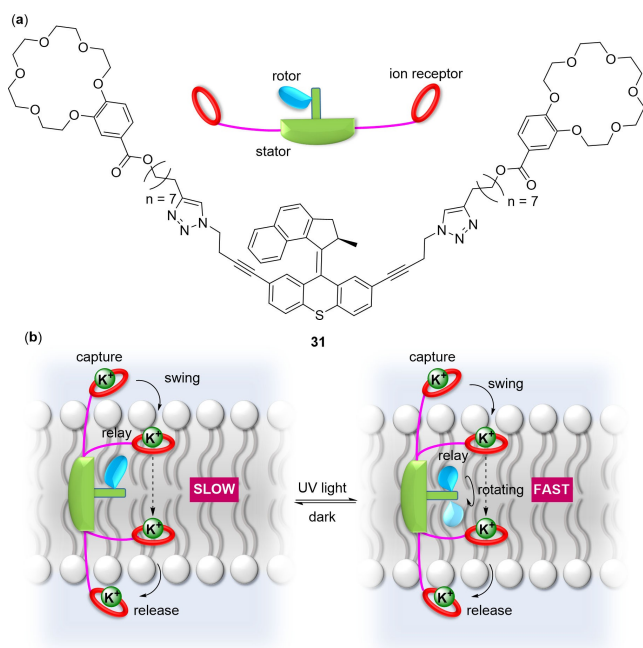


**Figure 22.** (a) Molecular structure of the molecular motor **31**. (b) Proposed mechanism for light-gated cation transport.

### 3.1. Controlling Membrane Permeability through Redox Reactions

The first studies towards demonstrating redox sensitive transport were focused on creating hydrophilic, water-soluble pro-transporters, incapable of entering the membrane until reduction by biological reducing agents (typically GSH) generates the active membrane-permeable transporter. Manna and co-workers demonstrated this concept using cationic, membrane impermeable tris-thiourea **32** (Figure 23).<sup>[52]</sup> The caged transporter exhibited minimal ion transport activity, in contrast to the neutral ionophore which exhibited effective chloride transport ( $EC_{50} = 580$  nM). GSH-mediated dealkylation of the sulfonium proceeded efficiently at cancerous cell concentrations of GSH (*ca.* 10 mM) but significantly slower at healthy cell concentrations (< 2 mM). Unfortunately, when the cytotoxicity of the transporter was tested in BHK-21, HeLa and MDCK cell lines, it

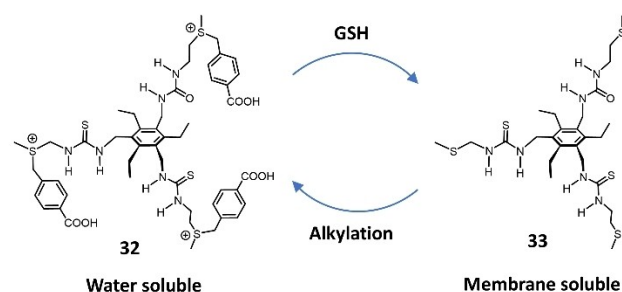


**Figure 23.** The GSH-mediated dealkylation of proanionophore **32** to form active chloride transporter **33**.

was revealed to be very low; this result highlights that anion transport alone is not always sufficient to induce toxicity and that the nature of the transporter is also a key consideration. The authors noted that the sulfonium moiety is attractive in the context of ion transporters not only because it is easily cleavable under physiological conditions, but also because it increases the cellular uptake of the transporter to a greater extent than other onium-based moieties, which is a key consideration for designing transporters as therapeutics.<sup>[53]</sup>

The same group followed up this work with related multi-stimuli responsive systems, including a thiourea-based chloride transporter which is alkylated with an *o*-nitrobenzylbenzoic acid group to create a membrane impermeable sulfonium species, which in turn could be dealkylated by UV light, GSH or reactive oxygen species (ROS) to regenerate the active chloride transporter.<sup>[54]</sup> The group's most recent publication in this area focused on a GSH and nitroreductase (NR) responsive pro-anionophore,<sup>[55]</sup> an enzyme overexpressed in hypoxic cells.

Employing a similar approach based on reductively enhancing the hydrophobicity of a pro-anionophore, Gabbai and co-workers reported the first examples of redox responsive sigma-hole bonding anion transporter.<sup>[56]</sup> The joint chalcogen and pnictogen bonding system **34** exploited sulfur and antimony centers to give a dicationic species, capable of strong binding to chloride via chalcogen and pnictogen bonding interactions ( $K_{CL} > 10^6$  M<sup>-1</sup>). Conversely, the reduced sulfide **35** exhibited a binding constant of *ca.*  $10^3$  M<sup>-1</sup>. Despite the weaker chloride affinity, the monocationic transporter **35** resulted in enhanced chloride transport when coupled with valinomycin (VM) compared to the dicationic species, which was rationalized by the increased hydrophilicity of the dicationic **34** impeding its membrane permeability, and potentially also due to its excessive binding strength inhibiting releasing of the chloride. When exposed to sub-physiological concentrations of GSH in situ, the sulfonium was rapidly reduced in 20 minutes to form the sulfide and thus the active transporter, as demonstrated by chloride ion-selective electrode experiments vesicles (Figure 24).

### 3.2. Redox-Controlled Ion Binding

An alternative strategy to develop redox-responsive transporters is to block the ion binding site with a redox labile protecting group. In this approach there is no major change in the membrane permeability. Talukdar and co-workers first demonstrated this concept by introducing a 2,4-dinitrobenzene sulfonyl (DNS) group to the known chloride channel-forming isophthalamide unit **36**, in order to inhibit its self-assembly into channels.<sup>[57]</sup> DNS is known to decompose in the presence of GSH to release the glutathione dinitrobenzene adduct and SO<sub>2</sub>, which is toxic to cells in high concentrations and thus provides a potential secondary trigger for cellular apoptosis (Figure 25).<sup>[58]</sup> The authors demonstrated reduced chloride transport in the DNS blocked isophthalamide **37** compared to uninhibited channel forming species **36**, and facile cleavage of the DNS group in

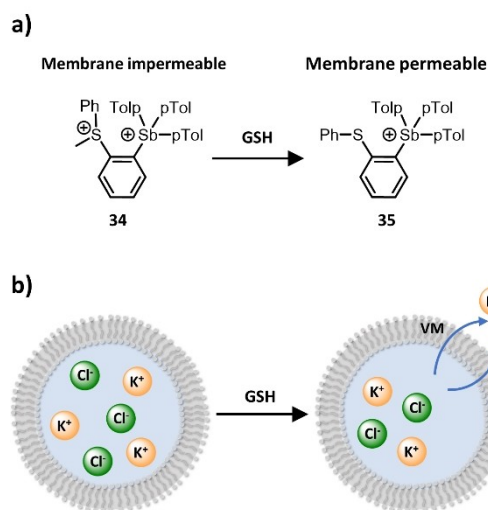


**Figure 24.** (a) GSH-mediated demethylation of pro-transporter **34**, yielding the active chloride transporter **35**. (b) Chloride efflux process from vesicles in the presence of valinomycin (VM).

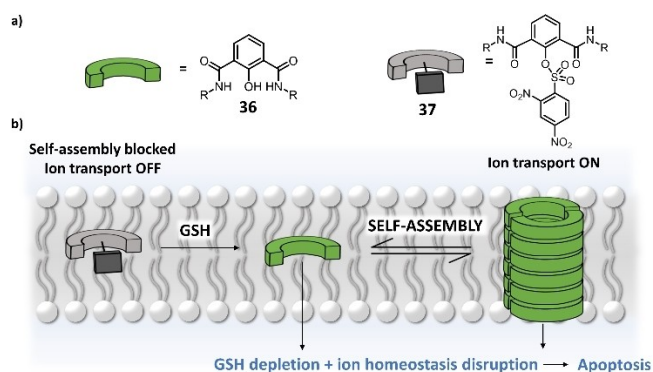


**Figure 25.** (a) Chloride channel forming isophthalamide **36** and the DNS-protected isophthalamide **37**. (b) Deprotection of DNS-isophthalamides **37** and the subsequent self-assembly to form a transmembrane chloride channel.

the presence of GSH to give activity almost identical to **36**. Cell viability studies on MCF-7 cells also revealed that protected chloride transporter **37** exhibited higher cytotoxicity than the free transporter. This was shown to be as a result of the DNS-protected compound's improved cell permeability, rather than the effect of released  $\text{SO}_2$  gas. Remarkably, when compared to the known anti-cancer agent doxorubicin, the DNS protected isophthalamides showed similar efficacy in inhibiting the proliferation of MCF-7 cells, thus indicating its potential to inhibit tumor growth in vivo.

Gale and co-workers reported a family of cycloaurated 1,3-bis(benzimidazole-2-yl)pyrimidine chloride transporters **38–43**, capable of redox-switchable anion transport (Figure 26).<sup>[59]</sup> Both gold chloride and gold N-heterocyclic carbene (NHC) complexes were investigated, with complexes **39** and **42** displaying minimal ion transport properties.

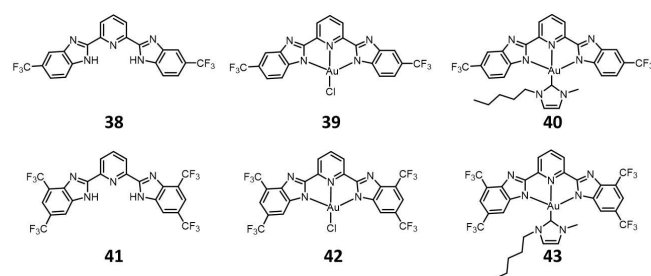


**Figure 26.** 1,3-bis(benzimidazole-2-yl)pyrimidine chloride transporters **38** and **41** and their cycloaurated analogues **39–43**.

Interestingly, the gold NHC complexes **40** and **43** showed non-trivial transport activity, which is attributed to the coordination of chloride or hydroxide to the metal center. When exposed to any of three reducing agents (dithiothreitol (DTT), tris(2-carboxyethyl) phosphine (TCEP) or GSH) rapid reduction of  $\text{Au}^{\text{III}}$  to  $\text{Au}^{\text{I}}$  could be achieved, thus deprotecting the binding site and generating the active chloride carrier. In situ deprotection experiments, both  $\text{Au}-\text{Cl}$  and  $\text{Au}-\text{NHC}$  complexes were found to give almost identical transport activities to their parent compounds in the presence of reducing agent. Cell viability studies on both cancerous and non-cancerous cell lines revealed that the cycloaurated complexes **40** and **42** exhibited lower cytotoxicity than their parent compounds in non-cancerous cell lines, attributed to lower GSH concentrations, and comparable toxicity to their parent compounds in cancerous cell lines. This indicates that the active chloride transporter is selectively regenerated in reductive cancerous environments. Complex **43**, however, showed increased cytotoxicity relative to the parent compound, postulated to be due to facile deprotection at low GSH concentrations.

### 3.3. Redox-Responsive Tellurium-Centered Transporters

The most recent class of redox sensitive systems to be reported in the literature are chalcogen bonding tellurium-based receptors. This is in part due to the range of Te oxidation states accessible using biologically relevant reductants and oxidants in aqueous conditions, in addition to their high polarizability and resultant strong chalcogen bonding capability. The first tellurium transporters reported were prepared by Gabbai and co-workers, comprising a small family of biaryl cationic tellurium transporters **44–49** methylated at the tellurium center (Figure 27).<sup>[60]</sup> These exhibited strong chloride binding, over four orders of magnitude stronger than their neutral counterparts, due to a combination of electrostatics and deepening of the  $\sigma$ -hole. Chloride transport experiments in vesicles revealed increased activity for the cationic tellurium systems relative to their neutral counterparts. However, the authors note this activity increase is not as significant as expected from binding data in solution, possibly due to the strong chloride binding inhibiting release from the transporter (the Goldilocks



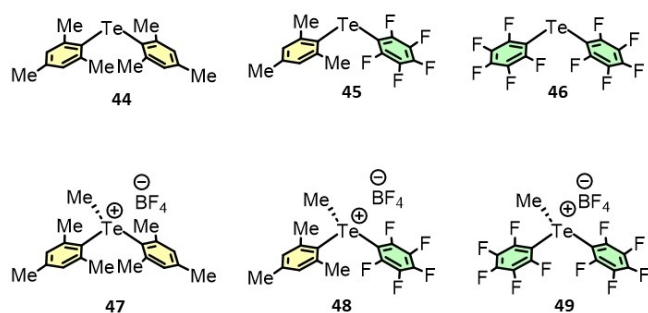


**Figure 27.** Gabbaï's biaryl telluride compounds **44–46**, and the corresponding cationic anionophores **47–49**.

effect),<sup>[61]</sup> or differing partitioning of the derivatives into the membrane.

The redox-responsive ion transporters discussed thus far are examples of irreversible OFF to ON switching. Recently Langton and co-workers reported a Te based ionophore capable of reversible switching in ON to OFF (and vice-versa), or OFF to ON to OFF multi-state switching modes.<sup>[62]</sup> This was achieved by careful control over the tellurium oxidation state in a small family of tellurium biaryl compounds, **50–55** (Figure 28a). The telluride and tellurone ( $\text{Te}^{\text{II}}$  and  $\text{Te}^{\text{VI}}$ , respectively) do not bind chloride, as revealed by NMR binding titrations, and are inactive transporters. In contrast, the telluroxide ( $\text{Te}^{\text{IV}}$ ) showed appreciable chloride affinity and excellent chloride transport ( $\text{EC}_{50} = 45 \text{ nM}$ ) in vesicles. These effects were justified by the enhanced Lewis acidity of the Te centre with oxidation state, whilst reduced steric accessibility of the anion to the tellurone due to the additional oxo-group was postulated to be responsive for the inhibited transport activity. The authors also prepared a related family of selenium biaryl

compounds, **53–55**, but observed no chloride binding by  $^1\text{H}$  NMR titration, consistent with the poorer chalcogen bonding affinity of the lighter chalcogen congeners. Switching of the tellurium oxidation state was achieved by treatment with either DTT (reduction),  $\text{H}_2\text{O}_2$  or cumene hyperoxide (oxidation) (Figure 28b), which could be achieved in an *in situ* fashion within the membrane. Careful control over stoichiometry allowed for precise switching between different Te oxidation states, enabling temporal control over ion transport in response to changing redox environment.

## 4. Conclusions

The past decade has witnessed a dramatic advance in the development of synthetic ion transport systems that respond to both photo- and redox-stimuli. These systems span both channels and carriers which are controlled by irreversible and reversible mechanisms. The field is now moving beyond proof-of-concept experiments, and beginning to look towards downstream applications in medicine, chemical biology, and nanotechnology. Stimuli-responsive transporters are anticipated to find application in targeted therapeutics, either for channelopathies or cancer. It is likely that light-activated systems could offer a useful approach towards spatio-temporal activation, while redox-regulated systems, activated by oxidizing or reducing cellular environments, may find utility in anticancer therapies. Beyond therapeutics, we also envisage applications in synthetic biology, in which readily addressable synthetic transporters can be used to facilitate the flow of molecules between synthetic cell compartments. Research in this area continues at pace, and we anticipate many exciting developments in the near future at the interface of synthetic supramolecular chemistry and biology.

## Acknowledgements

M. A., S. A. G. and M. J. L. thank the Leverhulme Trust (RPG-2020-130) for financial support. M. J. L. is a Royal Society University Research Fellow.

## Conflict of Interest

The authors declare no conflict of interest.

## Data Availability Statement

Data sharing is not applicable to this article as no new data were created or analyzed in this study.

**Keywords:** Anion Transport · Channels · Membranes · Photoswitches · Redox Reactions

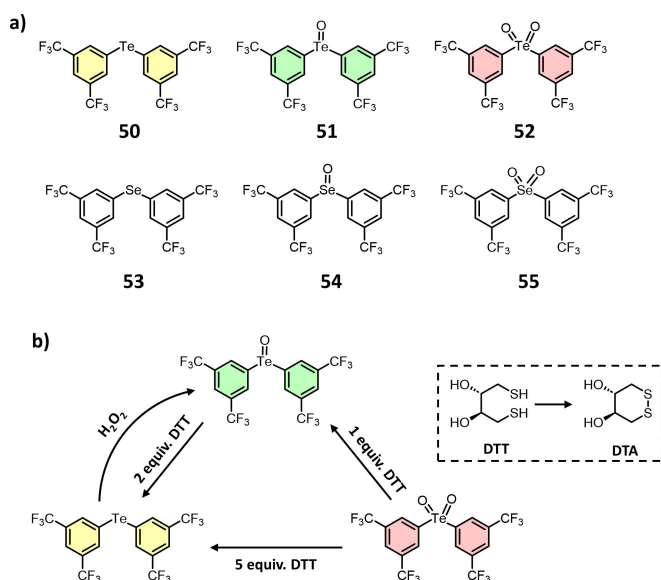


**Figure 28.** Reversibly controlled redox responsive ionophores (a) Biaryl tellurium species **50–52** and biaryl selenium species **53–55**. (b) Redox transformations between **50**, **51** and **52**.

- [1] a) J. T. Davis, P. A. Gale, R. Quesada, *Chem. Soc. Rev.* **2020**, *49*, 6056–6086; b) A. V. Jentzsch, S. Matile, *Halogen Bonding in Solution*, Wiley, Hoboken **2021**, pp. 195–231; c) J. T. Davis, O. Okunola, R. Quesada, *Chem. Soc. Rev.* **2010**, *39*, 3843–3862; d) A. Roy, P. Talukdar, *ChemBioChem* **2021**, *22*, 2925–2940; e) L. E. Bickerton, T. G. Johnson, A. Kerckhoffs, M. J. Langton, *Chem. Sci.* **2021**, *12*, 11252–11274; f) A. Barba-Bon, M. Nilam, A. Hennig, *ChemBioChem* **2020**, *21*, 886–910.
- [2] a) D. C. Gadsby, *Nat. Rev. Mol. Cell Biol.* **2009**, *10*, 344–352; b) E. Gouaux, R. MacKinnon, *Science* **2005**, *310*, 1461–1465.
- [3] a) M. M. Tedesco, B. Ghebremariam, N. Sakai, S. Matile, *Angew. Chem. Int. Ed.* **1999**, *38*, 540–543; b) P. Talukdar, G. Bollot, J. Mareda, N. Sakai, S. Matile, *Chem. Eur. J.* **2005**, *11*, 6525–6532; c) T. Muraoka, T. Endo, K. V. Tabata, H. Noji, S. Nagatoishi, K. Tsumoto, R. Li, K. Kinbara, *J. Am. Chem. Soc.* **2014**, *136*, 15584–15595.
- [4] N. Busschaert, R. B. P. Elmes, D. D. Czech, X. Wu, I. L. Kirby, E. M. Peck, K. D. Hendzel, S. K. Shaw, B. Chan, B. D. Smith, K. A. Jolliffe, P. A. Gale, *Chem. Sci.* **2014**, *5*, 3617.
- [5] a) X. Wu, J. Small, A. Cataldo, A. M. Withecombe, P. Turner, P. A. Gale, *Angew. Chem. Int. Ed.* **2019**, *58*, 15142–15147; b) W. Si, Z.-T. Li, J.-L. Hou, *Angew. Chem. Int. Ed.* **2014**, *53*, 4578–4581.
- [6] Y. R. Choi, B. Lee, J. Park, W. Namkung, K.-S. Jeong, *J. Am. Chem. Soc.* **2016**, *138*, 15319–15322.
- [7] M. J. Langton, *Nat. Chem. Rev.* **2021**, *5*, 46–61.
- [8] J. de Jong, J. E. Bos, S. J. Wezenberg, *Chem. Rev.* **2023**, *123*, 8530–8574.
- [9] a) N. Busschaert, M. Wenzel, M. E. Light, P. Iglesias-Hernández, R. Pérez-Tomás, P. A. Gale, *J. Am. Chem. Soc.* **2011**, *133*, 14136–14148; b) S.-K. Ko, S. K. Kim, A. Share, V. M. Lynch, J. Park, W. Namkung, W. Van Rossom, N. Busschaert, P. A. Gale, J. L. Sessler, I. Shin, *Nat. Chem.* **2014**, *6*, 885–892; c) T. Saha, M. S. Hossain, D. Saha, M. Lahiri, P. Talukdar, *J. Am. Chem. Soc.* **2016**, *138*, 7558–7567; d) C. Cossu, M. Fiore, D. Baroni, V. Capurro, E. Caci, M. Garcia-Valverde, R. Quesada, O. Moran, *Front. Pharmacol.* **2018**, *9*, <https://doi.org/10.3389/fphar.2018.00852>.
- [10] M. R. Banghart, M. Volgraf, D. Trauner, *Biochemistry* **2006**, *45*, 15129–15141.
- [11] A. Roy, A. Gautam, J. A. Malla, S. Sarkar, A. Mukherjee, P. Talukdar, *Chem. Commun.* **2018**, *54*, 2024–2027.
- [12] J. A. Malla, A. Roy, P. Talukdar, *Org. Lett.* **2018**, *20*, 5991–5994.
- [13] a) S. K. Choi, M. Verma, J. Silpe, R. E. Moody, K. Tang, J. J. Hanson, J. R. Baker, *Bioorg. Med. Chem.* **2012**, *20*, 1281–1290; b) G. Jalani, V. Tam, F. Vetrone, M. Cerruti, *J. Am. Chem. Soc.* **2018**, *140*, 10923–10931.
- [14] A. Koçer, M. Walko, W. Meijberg, B. L. Feringa, *Science* **2005**, *309*, 755–758.
- [15] C. Bao, M. Ma, F. Meng, Q. Lin, L. Zhu, *New J. Chem.* **2015**, *39*, 6297–6302.
- [16] S. B. Salunke, J. A. Malla, P. Talukdar, *Angew. Chem. Int. Ed.* **2019**, *58*, 5354–5358.
- [17] L. E. Bickerton, M. J. Langton, *Chem. Sci.* **2022**, *13*, 9531–9536.
- [18] R. F. Khairutdinov, J. K. Hurst, *Langmuir* **2004**, *20*, 1781–1785.
- [19] a) S. L. Oscurato, M. Salvatore, P. Maddalena, A. Ambrosio, *Nat. Photonics* **2018**, *7*, 1387–1422; b) V. Y. Chang, C. Fedele, A. Priimagi, A. Shishido, C. J. Barrett, *Adv. Opt. Mater.* **2019**, *7*, 1900091.
- [20] Y. R. Choi, G. C. Kim, H.-G. Jeon, J. Park, W. Namkung, K.-S. Jeong, *Chem. Commun.* **2014**, *50*, 15305–15308.
- [21] M. Ahmad, S. Metya, A. Das, P. Talukdar, *Chem. Eur. J.* **2020**, *26*, 8703–8708.
- [22] J. A. Peterson, C. Wijesooriya, E. J. Gehrman, K. M. Mahoney, P. P. Goswami, T. R. Albright, A. Syed, A. S. Dutton, E. A. Smith, A. H. Winter, *J. Am. Chem. Soc.* **2018**, *140*, 7343–7346.
- [23] A. Kerckhoffs, M. J. Langton, *Chem. Sci.* **2020**, *11*, 6325–6331.
- [24] A. Kerckhoffs, Z. Bo, S. E. Penty, F. Duarte, M. J. Langton, *Org. Biomol. Chem.* **2021**, *19*, 9058–9067.
- [25] D. Villarrón, S. J. Wezenberg, *Angew. Chem. Int. Ed.* **2020**, *59*, 13192–13202.
- [26] S. J. Wezenberg, L.-J. Chen, J. E. Bos, B. L. Feringa, E. N. W. Howe, X. Wu, M. A. Siegler, P. A. Gale, *J. Am. Chem. Soc.* **2022**, *144*, 331–338.
- [27] a) Z. Kokan, M. J. Chmielewski, *J. Am. Chem. Soc.* **2018**, *140*, 16010–16014; b) D. A. Leigh, V. Marcos, T. Nalbantoglu, I. J. Vitorica-Yrezabal, F. T. Yasar, X. Zhu, *J. Am. Chem. Soc.* **2017**, *139*, 7104–7109.
- [28] M. Ahmad, S. Chattopadhyay, D. Mondal, T. Vijayakanth, P. Talukdar, *Org. Lett.* **2021**, *23*, 7319–7324.
- [29] M. Ahmad, D. Mondal, N. J. Roy, T. Vijayakanth, P. Talukdar, *ChemPhotoChem* **2022**, *6*, e202200002.
- [30] R.-Y. Yang, C. Bao, Q.-N. Lin, L.-Y. Zhu, *Chin. Chem. Lett.* **2015**, *26*, 851–856.
- [31] T. Liu, C. Bao, H. Wang, Y. Lin, H. Jia, L. Zhu, *Chem. Commun.* **2013**, *49*, 10311–10313.
- [32] a) C. Li, H. Chen, Q. Chen, H. Shi, X. Yang, K. Wang, J. Liu, *Anal. Chem.* **2020**, *92*, 10169–10176; b) M. Debnath, S. Chakraborty, Y. P. Kumar, R. Chaudhuri, B. Jana, J. Dash, *Nat. Commun.* **2020**, *11*, 469.
- [33] a) X. Wang, J. Huang, Y. Zhou, S. Yan, X. Weng, X. Wu, M. Deng, X. Zhou, *Angew. Chem. Int. Ed.* **2010**, *49*, 5305–5309; b) G. F. Luo, Y. Biniuri, W. H. Chen, J. Wang, E. Neumann, H. B. Marjault, R. Nechushtai, M. Winkler, T. Happe, I. Willner, *Angew. Chem. Int. Ed.* **2020**, *59*, 9163–9170; c) M. Nishio, K. Tsukakoshi, K. Ikebukuro, *Biosens. Bioelectron.* **2021**, *178*, 113030.
- [34] P. Li, G. Xie, X.-Y. Kong, Z. Zhang, K. Xiao, L. Wen, L. Jiang, *Angew. Chem. Int. Ed.* **2016**, *55*, 15637–15641.
- [35] C. Li, H. Chen, X. Yang, K. Wang, J. Liu, *Chem. Commun.* **2021**, *57*, 8214–8217.
- [36] Y. Zhou, Y. Chen, P.-P. Zhu, W. Si, J.-L. Hou, Y. Liu, *Chem. Commun.* **2017**, *53*, 3681–3684.
- [37] S. P. H. Alexander, A. Mathie, J. A. Peters, *Br. J. Pharmacol.* **2011**, *164*, S115–S135.
- [38] L. Husaru, M. Gruner, T. Wolff, W. D. Habicher, R. Salzer, *Tetrahedron Lett.* **2005**, *46*, 3377–3379.
- [39] L. Husaru, R. Schulze, G. Steiner, T. Wolff, W. D. Habicher, R. Salzer, *Anal. Bioanal. Chem.* **2005**, *382*, 1882–1888.
- [40] L. Lien, D. C. J. Jaikaran, Z. Zhang, G. A. Woolley, *J. Am. Chem. Soc.* **1996**, *118*, 12222–12223.
- [41] P. V. Jog, M. S. Gin, *Org. Lett.* **2008**, *10*, 3693–3696.
- [42] T. J. Huang, B. K. Juluri, *Nanomedicine* **2008**, *3*, 107–124.
- [43] S. Erbas-Cakmak, D. A. Leigh, C. T. McTernan, A. L. Nussbaumer, *Chem. Rev.* **2015**, *115*, 10081–10206.
- [44] a) C. O. Dietrich-Buchecker, M. C. Jimenez-Molero, V. Sartor, J. P. Sauvage, *Pure Appl. Chem.* **2003**, *75*, 1383–1393; b) E. Moulin, L. Faour, C. C. Carmona-Vargas, N. Giuseppone, *Adv. Mater.* **2020**, *32*, 1906036.
- [45] S. Chen, Y. Wang, T. Nie, C. Bao, C. Wang, T. Xu, Q. Lin, D. H. Qu, X. Gong, Y. Yang, L. Zhu, H. Tian, *J. Am. Chem. Soc.* **2018**, *140*, 17992–17998.
- [46] C. Wang, S. Wang, H. Yang, Y. Xiang, X. Wang, C. Bao, L. Zhu, H. Tian, D.-H. Qu, *Angew. Chem. Int. Ed.* **2021**, *60*, 14836–14840.
- [47] T. G. Johnson, A. Sadeghi-Kelishadi, M. J. Langton, *J. Am. Chem. Soc.* **2022**, *144*, 10455–10461.
- [48] D. Roke, S. J. Wezenberg, B. L. Feringa, *Proc. Natl. Acad. Sci. USA* **2018**, *115*, 9423–9431.

- [49] V. García-López, F. Chen, L. G. Nilewski, G. Duret, A. Aliyan, A. B. Kolomeisky, J. T. Robinson, G. Wang, R. Pal, J. M. Tour, *Nature* **2017**, *548*, 567–572.
- [50] W.-Z. Wang, L.-B. Huang, S.-P. Zheng, E. Moulin, O. Gavet, M. Barboiu, N. Giuseppone, *J. Am. Chem. Soc.* **2021**, *143*, 15653–15660.
- [51] H. Yang, J. Yi, S. Pang, K. Ye, Z. Ye, Q. Duan, Z. Yan, C. Lian, Y. Yang, L. Zhu, D.-H. Qu, C. Bao, *Angew. Chem. Int. Ed.* **2022**, *61*, e202204605.
- [52] N. Akhtar, N. Pradhan, A. Saha, V. Kumar, O. Biswas, S. Dey, M. Shah, S. Kumar, D. Manna, *Chem. Commun.* **2019**, *55*, 8482–8485.
- [53] a) B. Díaz de Greñu, P. I. Hernández, M. Espona, D. Quiñero, M. E. Light, T. Torroba, R. Pérez-Tomás, R. Quesada, *Chem. Eur. J.* **2011**, *17*, 14074–14083; b) S. Cournoyer, A. Addiou, A. Belounis, M. Beaunoyer, C. Nyalendo, R. Le Gall, P. Teira, E. Haddad, G. Vassal, H. Sartelet, *BMC Cancer* **2019**, *19*, 1018.
- [54] S. Das, O. Biswas, N. Akhtar, A. Patel, D. Manna, *Org. Biomol. Chem.* **2020**, *18*, 9246–9252.
- [55] N. Akhtar, O. Biswas, D. Manna, *Org. Biomol. Chem.* **2021**, *19*, 7446–7459.
- [56] G. Park, F. P. Gabbai, *Chem. Sci.* **2020**, *11*, 10107–10112.
- [57] a) X. Li, B. Shen, X.-Q. Yao, D. Yang, *J. Am. Chem. Soc.* **2007**, *129*, 7264–7265; b) J. A. Malla, R. M. Umesh, S. Yousf, S. Mane, S. Sharma, M. Lahiri, P. Talukdar, *Angew. Chem. Int. Ed.* **2020**, *59*, 7944–7952.
- [58] J. Liu, Y. Huang, S. Chen, C. Tang, H. Jin, J. Du, *Oxid. Med. Cell. Longevity* **2016**, *2016*, 4529060.
- [59] M. Fares, X. Wu, D. Ramesh, W. Lewis, P. A. Keller, E. N. W. Howe, R. Pérez-Tomás, P. A. Gale, *Angew. Chem. Int. Ed.* **2020**, *59*, 17614–17621.
- [60] B. Zhou, F. P. Gabbai, *Chem. Sci.* **2020**, *11*, 7495–7500.
- [61] M. Kirch, J.-M. Lehn, *Angew. Chem. Int. Ed.* **1975**, *14*, 555–556.
- [62] A. Docker, T. G. Johnson, H. Kuhn, Z. Zhang, M. J. Langton, *J. Am. Chem. Soc.* **2023**, *145*, 2661–2668.

Manuscript received: June 23, 2023

Accepted manuscript online: July 21, 2023

Version of record online: August 3, 2023